

# Double-K parameters and the cohesive-stress-based $K_R$ curve for the negative geometry

Shilang Xu

*Department of Civil Engineering, Dalian University of Technology, Dalian 116024, China*  
slxu@dlut.edu.cn

Hans W. Reinhardt

*Institute of Construction Materials, University of Stuttgart, D-70550 Stuttgart, Germany*  
reinhardt@iwb.uni-stuttgart.de

**ABSTRACT:** In this paper, the fictitious crack distributed with softening cohesive stress in the case of the infinite plate with a semi-infinite crack, as an example of negative fracture geometry was analytically solved and numerically studied. Using the analytical solutions and numerical results both double-K parameters and cohesive stress based  $K_R$  curve were determined. The gained results show that there exist crack initiation, crack propagation until maximum load was exceeded and the crack retrenches slowly after maximum load. The three-parameter law of fracture toughness increase exists yet in such negative geometry. Therefore, the double-K fracture model applies to the negative geometry too. The net stress intensity factor at the propagating crack tip is larger than 60% of the total stress intensity factor caused by the externally applied load. It implies that a zero net stress intensity factor at the fictitious crack tip does not exist in the case of negative geometry.

**Key words:** negative geometry, fictitious crack, double-K model, cohesive stress based  $K_R$  curve, net stress intensity factor, crack propagation

## 1 INTRODUCTION

The case of an infinite plate with a semi-infinite crack belongs to negative fracture geometry in fracture mechanics. In order to research whether the double-K fracture model (Xu & Reinhardt 1999a, b, c; Xu & Reinhardt 2000) and the cohesive stress based crack extension resistance curve method (Xu & Reinhardt 1998) apply to the negative geometry, one has to seek the analytical solution of the fictitious crack model and the analytical expressions of the cohesive stress based crack extension resistance during the complete fracture process for the semi-infinite crack as the theoretical basis for numerical and experimental studies.

The double-K fracture model has been successfully applied to three-point bending notched beams, CT specimens and WS specimens (Xu & Reinhardt 1999 b, c; Xu & Reinhardt 2000), such positive fracture geometry. In this

paper, an attempt is made to find the analytical solution of the stress intensity factors at the fictitious crack tip during the different states of crack propagation in the semi-infinite crack for concrete and give the mathematical expressions of them for the different states of crack propagation.

Furthermore, numerical simulation on a big size concrete plate with the dimensions of 4m times 4m has been performed using a nonlinear finite element code based on micro-plane model for gaining the plots of load versus loading point displacement ( $P-\delta$ ), load versus crack propagation length ( $P-\Delta a$ ) and load versus crack tip opening displacement ( $P-CTOD$ ). Based on these data, double-K parameters and the cohesive stress based  $K_R$  curve were determined using the analytical solution according to the corresponding propagated crack length. The corresponding net stress intensity factor for the complete fracture process is calculated, too. The gained results provide new understanding for the application of the double-K fracture model to the negative geometry.

## 2 THE ANALYTICAL SOLUTIONS OF A SEMI-INFINITE CRACK WITH A FICTITIOUS CRACK ZONE IN AN INFINITE PLATE

Herein, an infinite plate of unit thickness with a semi-infinite crack subjected to a pair of splitting forces  $P$  acting against the crack surfaces at the position  $y = 0, x = -(b + \Delta a)$  where  $\Delta a \geq 0$  at an arbitrary loading state in a moving Cartesian coordinate is shown in Fig. 1 (a). The moving Cartesian coordinate is assumed to be fixed at the tip of propagating crack and to be moved forward ahead with the crack propagation. With increase of the acting forces  $P$  the corresponding  $P$ - $\delta$  curve and  $P$ - $\Delta a$  curve will follow the patterns shown in Fig. 1 (b) and (c) respectively.

We can assume that when the acting force  $P$  is less than  $P_{ini}$ , the  $P$ - $\delta$  curve will be straight and there will be no occurrence of stable crack growth.

At this loading state for  $\Delta a = 0$ , the stress intensity factor at the preformed crack tip can be calculated as follows (Tada et al., 1985):

$$K_I = K_I^E = \sqrt{\frac{2}{\pi}} \frac{P}{\sqrt{b}} \quad (P \leq P_{ini}) \quad (1)$$

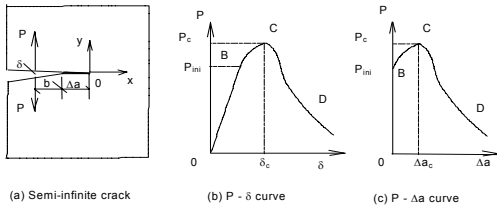


Fig. 1. The semi-infinite crack extension in quasi-brittle materials.

Once the acting force  $P$  exceeds the value of  $P_{ini}$ , the  $P$ - $\delta$  curve will be nonlinear and stable crack propagation will occur. In concrete, the upper and lower surfaces of a propagating crack are not stress-free when its width at the preformed crack tip is less than  $w_0$ . The crack propagation occurred in the region to be restrained by the cohesive stress in the region to be restrained by the cohesive stress was termed the "fictitious crack". Therefore, our main attention is focused on finding a closed form solution of the semi-infinite crack with a fictitious crack zone in an infinite plate after the acting force  $P$  exceeded the value of  $P_{ini}$ .

For convenience to solve the problem as mentioned above, the original point of the Cartesian coordinates is fixed on the fictitious crack tip and can be moved with the development of the fictitious crack. Therefore, the considered semi-infinite crack with a fictitious crack zone subjected to one pair of the splitting forces  $P$  in the

infinite plate is demonstrated in Fig. 2 (a). According to the superposition assumption the crack problem shown in Fig. 2 (a) can be divided into two crack problems shown in Fig. 2 (b) and (c) separately.

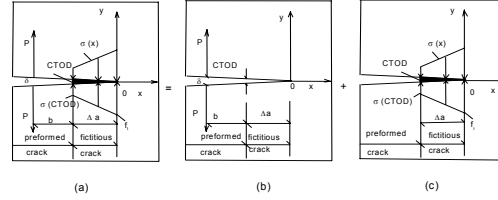


Fig. 2 The superposition demonstration of a semi-infinite crack with a fictitious crack zone in an infinite plate subjected to a pair of splitting forces  $P$  acting against the crack surfaces at the position  $y = 0, x = -(b + \Delta a)$ .

From the solution presented in formula (1) we can easily obtain the solution for the crack problem illustrated in Fig. 2 (b) as follows:

$$K_I^E = \sqrt{\frac{2}{\pi}} \frac{P}{\sqrt{b + \Delta a}} \quad (P > P_{ini}) \quad (2)$$

The stress intensity factor  $K_{Ic}$  due to the cohesive stress on the fictitious crack zone shown in Fig. 2 (c) can be calculated through integrating equation (1):

$$K_I^c = \int_{-\Delta a}^0 \sqrt{\frac{2}{\pi}} \frac{\sigma(x) dx}{\sqrt{-x}} \quad (3)$$

Because the cohesive stress distributions  $\sigma(x)$  along the fictitious crack zone are different at the various crack propagation states, the solution of integration (3) for each state will be given subsequently.

Since  $\sigma$ - $w$  curves can be taken as material properties, the cohesive stress distribution on the fictitious crack can be determined by comparing CTOD in different loading states with the characteristic coordinates of the bilinear softening curve,  $w_s$  and  $w_0$ . In fact, the cohesive stress is dependent on the crack profile. The distribution of

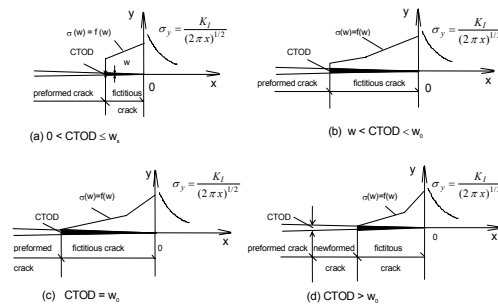


Fig. 3. Cohesive stress distributions on the fictitious crack at different loading states.

it is somewhat nonlinear. However, in order to be able to find an analytical solution for the problem and to have a good approximation for the solution, the cohesive stress on the fictitious crack is assumed to be a bilinear one. The cohesive stress distributions at the typical loading states corresponding to CTOD are demonstrated in Fig. 3. Now, the stress intensity factor due to the cohesive stress is solved in the following space for the different crack propagation states.

### 2.1 The stress intensity factor due to the trapezoid distribution of the cohesive stress on the fictitious crack when $0 \leq CTOD \leq CTOD_c$ (included critical situation)

It is known that a trapezoid distribution of the cohesive stress on the fictitious crack should be assumed if the loading state is in between point B and C shown in Fig. 1 (b) and (c) at which CTOD will satisfy the conditions of  $0 \leq CTOD \leq CTOD_c$ . For the semi-infinite crack with a fictitious crack zone in an infinite plate, the trapezoid distribution of the cohesive stress is illustrated in Fig. 4.

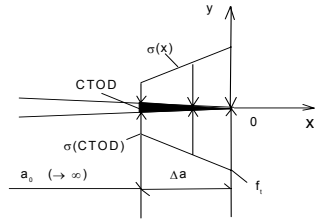


Fig. 4. The trapezoid distribution of the cohesive stress on the fictitious crack in a semi-infinite crack problem when  $0 \leq CTOD \leq CTOD_c$ .

And the corresponding expression of the cohesive stress distribution is as follows:

$$\sigma(x) = \sigma(CTOD) + [f_t - \sigma(CTOD)] \frac{\Delta a + x}{\Delta a} \quad -\Delta a \leq x \leq 0 \quad (4)$$

To submit equation (4) into integral (3) the stress intensity factor at the fictitious crack tip due to the cohesive stress for the crack problem shown in Fig. 4 can be received:

$$K_I^c = -\frac{2}{3} \sqrt{\frac{2}{\pi}} [2 f_t + \sigma(CTOD)] \sqrt{\Delta a} \quad (5)$$

### 2.2 The stress intensity factor due to the trapezoid bilinear distribution of the cohesive when $CTOD_c < CTOD < w_0$

After the external splitting forces P exceeded the maximum forces (critical forces)  $P_{max}$ , due to the softening properties of fictitious crack in concrete,

the P- $\delta$  curve follows a descending branch (see Fig. 1 (b)). If the CTOD is in such a region of  $CTOD_c < CTOD < w_0$ , according to the illustration of Fig. 3(b), the cohesive stress distribution on the fictitious crack should be a trapezoid bilinear distribution (Fig. 5).

The trapezoid bilinear distribution is expressed as follows:

$$\sigma(x) = \begin{cases} \sigma_1(x) = \sigma(CTOD) + [\sigma_s(CTOD_c) - \sigma(CTOD)] \frac{\Delta a + x}{\Delta a - \Delta a_c} & -\Delta a \leq x \leq -\Delta a_c \\ \sigma_2(x) = \sigma_s(CTOD_c) + [f_t - \sigma_s(CTOD_c)] \frac{\Delta a_c + x}{\Delta a_c} & -\Delta a_c \leq x \leq 0 \end{cases} \quad (6)$$

Similarly, to submit the expression of  $\sigma(x)$  into integral expression (3),  $K_{Ic}$  can be divided into two parts:

$$K_I^c = K_I^{c(1)} + K_I^{c(2)} = \int_{-\Delta a}^{-\Delta a_c} \sqrt{\frac{2}{\pi}} \frac{\sigma_1(x) dx}{\sqrt{-x}} + \int_{-\Delta a_c}^0 \sqrt{\frac{2}{\pi}} \frac{\sigma_2(x) dx}{\sqrt{-x}} \quad (7)$$

To integrate the two parts of equation (7) separately, one can get the detailed expressions of  $K_{Ic}^{(1)}$  and  $K_{Ic}^{(2)}$  as follows:

$$K_I^{c(1)} = -2 \sqrt{\frac{2}{\pi}} \left\{ \sigma(CTOD) [\sqrt{\Delta a} - \sqrt{\Delta a_c}] - \frac{1}{3} [\sigma_s(CTOD_c) - \sigma(CTOD)] \sqrt{\Delta a_c} + \frac{2}{3} \frac{\Delta a}{\sqrt{\Delta a} + \sqrt{\Delta a_c}} [\sigma_s(CTOD_c) - \sigma(CTOD)] \right\}$$

$$K_I^{c(2)} = -\frac{2}{3} \sqrt{\frac{2}{\pi}} [2 f_t + \sigma_s(CTOD_c)] \sqrt{\Delta a_c}$$

By combining them, the stress intensity factor due to the trapezoid bilinear cohesive stress distribution on the fictitious crack for the semi-infinite crack problem shown in Fig. 5 can be obtained:

$$K_I^c = -2 \sqrt{\frac{2}{\pi}} \left\{ \sigma(CTOD) [\sqrt{\Delta a} - \sqrt{\Delta a_c}] + \frac{1}{3} [2 f_t + \sigma(CTOD)] \sqrt{\Delta a_c} + \frac{2}{3} \frac{\Delta a}{\sqrt{\Delta a} + \sqrt{\Delta a_c}} [\sigma_s(CTOD_c) - \sigma(CTOD)] \right\} \quad (8)$$

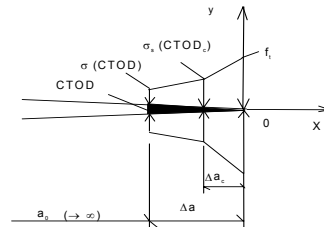


Fig. 5. The trapezoid bilinear distribution of the cohesive stress on the fictitious crack in the semi-infinite crack problem when  $CTOD_c < CTOD < w_0$  is met.

### 2.3 The stress intensity factor due to the fully bilinear cohesive stress distribution on the fictitious crack

For a special situation shown in Fig. 3(c) at which CTOD reaches the characteristic coordinate  $w_0$  of the  $\sigma$ - $w$  softening curve, a fully bilinear cohesive stress distribution on the fictitious crack should appear, see Fig. 6.

The corresponding expressions of the cohesive stress distribution are given as follows:

$$\sigma(x) = \begin{cases} \sigma_s(x) = \sigma_s(CTOD_c) \frac{\Delta a + x}{\Delta a - \Delta a_c} & -\Delta a \leq x \leq -\Delta a_c \\ \sigma_s(x) = \sigma_s(CTOD_c) + [f_i \cdot \sigma_s(CTOD_c)] \frac{\Delta a_c + x}{\Delta a_c} & -\Delta a \leq x \leq 0 \end{cases} \quad (9)$$

If one notes such a reason that the cohesive stress boundary conditions in the crack problem shown in Fig. 6 just is a special situation of that shown in Fig. 5, it has no need to submit expression (9) into integral (3) to carry out the complicated integration again. We only need to let  $\sigma(CTOD) = 0$ , and  $\Delta a = \Delta a_{w0}$  in integral (3), the stress intensity factor due to the fully bilinear cohesive stress on the fictitious crack zone shown in Fig. 6 can be easily obtained:

$$K_I^c = -\frac{4}{3} \sqrt{\frac{2}{\pi}} \left\{ f_i \sqrt{\Delta a_c} + \frac{\Delta a_c}{\Delta a_{w0} - \Delta a_c} \sigma_s(CTOD_c) \left[ \sqrt{\Delta a_{w0}} - \sqrt{\Delta a_c} \right] \right\} \quad (10)$$

The solution presented in expression (10) of  $K_{Ic}$  is also suitable for such a situation in which a new formed free crack has appeared and CTOD has exceeded the value of  $w_0$ . The reason is that for such a semi-infinite crack problem, the length of the preformed crack is infinite and the solutions of the stress intensity factor due to the cohesive stress boundary conditions corresponding to the situation shown in Fig. 3 (c) are the same as those shown in Fig. 3 (d).

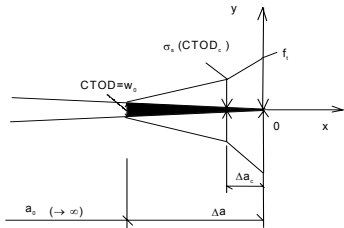


Fig. 6. The full bilinear distribution of the cohesive stress on the fictitious crack in the semi-infinite crack problem at a special situation of which CTOD =  $w_0$  is met.

### 3. THE EXPRESSIONS OF DOUBLE-K FRACTURE PARAMETERS, COHESIVE STRESS BASED $K_R$ CURVE AND THE NET STRESS INTENSITY FACTOR FOR NEGATIVE GEOMETRY

The double-K fracture parameters, i.e.  $K_{Ic}^{ini}$  and  $K_{Ic}^{un}$ , which were introduced in the double-K fracture model, are based on the form of stress intensity factor  $K$ .

One parameter  $K_{Ic}^{ini}$  is the initiation toughness that describes the crack initiation. Theoretically speaking, the initiation toughness  $K_{Ic}^{ini}$  is defined as the initial cracking stress intensity factor at the initial crack tip by the initial cracking load. So, for this kind of negative geometry, it is expressed as follows:

$$K_{Ic}^{ini} = K_I(P_{ini}, b_0) = \sqrt{\frac{2}{\pi}} \frac{P_{ini}}{\sqrt{b_0}} \quad (11)$$

In fact, the initiation toughness  $K_{Ic}^{ini}$  is the inherent toughness of a material. It implies that a crack does not propagate when the stress intensity factor at the initial crack tip is less than the inherent toughness, i.e., the initiation toughness  $K_{Ic}^{ini}$ .

Another parameter  $K_{Ic}^{un}$  is the critical stress intensity factor that describes the critical situation of unstable fracture. According to the definition, it meets,  $b = b_0 + \Delta a_c$ ,  $P = P_c$ . So, for calculating the value of  $K_{Ic}^{un}$  one only needs to submit  $P_c$  and  $b$  into the same formula (3). It is expressed as follows:

$$K_{Ic}^{un} = K_I(P_c, b_0 + \Delta a_c) = \sqrt{\frac{2}{\pi}} \frac{P_c}{\sqrt{b_0 + \Delta a_c}} \quad (12)$$

Until occurrence of the critical fracture, the toughness of a loaded body increases from the value of  $K_{Ic}^{ini}$  to the one of  $K_{Ic}^{un}$  due to the stable crack propagation. The increase of the toughness during the stable crack propagation is only due to the cohesive stress on the fictitious crack. The contribution due to cohesive stress at the critical situation is called  $K_{Ic}^c$ . In positive geometry, like three point notched bending beams, CT specimens, WS specimens, it was found that the increase of fracture toughness due to the cohesive stress during the crack propagation meets three-parameter law (Xu & Reinhardt 1999c; Xu & Reinhardt 2000), it applies:

$$K_{Ic}^{ini} + K_{Ic}^c = K_{Ic}^{un} \quad (13)$$

Contrarily for the considered negative geometry, from formulae (12) and (13), one can see that the stress intensity factor at the propagating crack tip decreases with the increase of crack length when the externally applied load remains constant. Whether the double-K model also applies to negative geometry is questionable yet.

In fact, a crack in the negative geometry once initiates, the length of the crack will increase until the externally applied load arrives at its maximum value  $P_{max}$ . During the crack propagation from

crack initiation to the load exceeding its maximum value, the stress intensity factor at the propagating crack tip not only depends on the crack extension, but also is strongly influenced by the increased externally applied load. Exactly speaking, it decreases with extension of the crack, and increases with the increase of the externally applied load  $P$ . However, whether the stress intensity factor actually increases or decreases depends whether  $(P/P_{ini})^2$  is larger than  $b/b_0$  or not. Concerning so big difference between the negative geometry and the positive one, we have to use numerical studies or experimental investigations to check how to calculate the critical stress intensity factor  $K_{Ic}^{un}$ . It means that one has to choose correctly the critical fracture state, i.e., correspondingly the critical crack length and the critical load  $P_c$ . Furthermore, in order to certify whether the double-K fracture model applies to the negative geometry, we need to confirm the difference between the values of  $K_{Ic}^{ini}$  and  $K_{Ic}^{un}$  due to the stable crack propagation is positive or negative. If it is positive, we also need to know whether this value is equal to the value of  $K_{Ic}^c$  contributed by the cohesive stress on the fictitious crack zone. Corresponding to several crack propagation states, the formulae to calculate the  $K_{Ic}^c$  are given in formulae (5), (8) and (10) respectively.

According to the definition of the cohesive stress based  $K_R$  curve (Xu & Reinhardt 1998), the analytical expressions of it for this negative geometry can be gained. For various different crack propagation states, the expressions are different. Corresponding expressions for each crack propagation state are given as follows respectively.

1. When  $CTOD \leq CTOD_c$  and  $\Delta a \leq \Delta a_c$ , it applies

$$K_R = K_{Ic}^{ini} + \frac{2}{3} \sqrt{\frac{2}{\pi}} (2 + \beta) \sqrt{\Delta a} f_t \quad (14)$$

2. When  $CTOD_c < CTOD \leq w_0$  and  $\Delta a_c < a \leq \Delta a_{w0}$ , we have

$$K_R = K_{Ic}^{ini} + 2 \sqrt{\frac{2}{\pi}} \left\{ \beta (\sqrt{\Delta a} - \sqrt{\Delta a_c}) + \frac{1}{3} (2 + \beta) \sqrt{\Delta a_c} + \frac{2}{3} \frac{\Delta a}{\sqrt{\Delta a} + \sqrt{\Delta a_c}} (\beta_s - \beta) \right\} f_t \quad (15)$$

3. When  $CTOD \geq w_0$  and  $\Delta a \geq \Delta a_{w0}$ , we have

$$K_R = K_{Ic}^{ini} + \frac{4}{3} \sqrt{\frac{2}{\pi}} \left\{ \sqrt{\Delta a_c} + \frac{\Delta a_{w0}}{\Delta a_{w0} - \Delta a_c} \beta_s (\sqrt{\Delta a_{w0}} - \sqrt{\Delta a_c}) \right\} f_t \quad (16)$$

where

$$\beta = \sigma(CTOD) / f_t \quad \text{and} \quad (17)$$

$$\beta_s = \sigma_s(CTOD_c) / f_t$$

Where  $CTOD$  is crack opening tip displacement and  $CTOD_c$  is its critical value;  $f_t$  is the tensile strength;  $\sigma(CTOD)$  can be determined according to the softening traction versus separation law of the concrete. A bilinear one also can be used, the corresponding parameters used in the bilinear softening traction-separation law have been coded in the CEB-FIP Model Code 1990.

For knowing whether the net stress intensity factor at the propagating crack tip meets a zero assumption used by some researchers, or not, we also calculated the net stress intensity factor at the propagating crack tip during the complete fracture process for this negative geometry in this paper. So, under common action of the externally applied load and the cohesive stress on the fictitious crack zone, the net stress intensity factor for this negative geometry for various crack propagation states can be easily expressed respectively as follows:

4. When  $CTOD \leq CTOD_c$  and  $\Delta a \leq \Delta a_c$ , it is

$$K_N = \sqrt{\frac{2}{\pi}} \frac{P}{\sqrt{b_0 + \Delta a}} - \frac{2}{3} \sqrt{\frac{2}{\pi}} (2 + \beta) \sqrt{\Delta a} f_t \quad (18)$$

5. When  $CTOD_c < CTOD \leq w_0$  and  $\Delta a_c < \Delta a \leq \Delta a_{w0}$ , it does

$$K_N = \sqrt{\frac{2}{\pi}} \frac{P}{\sqrt{b_0 + \Delta a}} - 2 \sqrt{\frac{2}{\pi}} \left\{ \beta (\sqrt{\Delta a} - \sqrt{\Delta a_c}) + \frac{1}{3} (2 + \beta) \sqrt{\Delta a_c} + \frac{2}{3} \frac{\Delta a}{\sqrt{\Delta a} + \sqrt{\Delta a_c}} (\beta_s - \beta) \right\} f_t \quad (19)$$

6. When  $CTOD \geq w_0$  and  $\Delta a \geq \Delta a_{w0}$ ,

$$K_N = \sqrt{\frac{2}{\pi}} \frac{P}{\sqrt{b_0 + \Delta a}} - \frac{4}{3} \sqrt{\frac{2}{\pi}} \left\{ \sqrt{\Delta a_c} + \frac{\Delta a_{w0}}{\Delta a_{w0} - \Delta a_c} \beta_s (\sqrt{\Delta a_{w0}} - \sqrt{\Delta a_c}) \right\} f_t \quad (20)$$

Using the formulae (5), (8) and (10) to (20) in this section and the former section, the double-K parameters, three-parameter law, cohesive stress based  $K_R$  curve and the net stress intensity factor during the complete fracture process for this negative geometry can be evaluated. For gaining the corresponding data, numerical studies or experiments on an infinite plate with a semi-infinite crack in mathematical meaning should be performed. Considering much expense carrying out the experiments on the infinite plate with a semi-infinite crack, the numerical studies should be firstly done. In the next section, the consequences gained from numerical studies will be shown and discussed.

#### 4. NUMERICAL INVESTIGATIONS AND THE GAINED RESULTS

In order to investigate the fracture behavior, numerical simulation for a concrete plate with plane dimensions of  $4000 \times 4000 \text{ mm}^2$  was performed using a nonlinear finite element code based on the micro-plane model (Ozbolt et al. 2001). In the finite element code, the micro-plane model was used for concrete material model and a fitting nonlinear softening traction-separation law and the crack band model (Bazant et al. 1983) were used for describing the fracture process zone (FPZ). Total elements are 4210. The preformed crack is 2000 mm long and the crack tip coordinates are in the centre of the plate. A pair of point loads act on two sides of the crack with a distance of 57.14 mm to the crack tip. The distance of acting loads to the crack tip is less than  $1/35$  of the total crack length and the ligament length. Therefore, this case should be considered as an infinite plate with a semi infinite crack case. In the calculation, the input data of material properties are that elastic modulus is 32 GPa, compressive strength is 40 MPa, tensile strength is 3.0 MPa and Poisson ratio is 0.18.

Through the numerical simulation, the gained plots of  $P$ - $\delta$ , CTOD- $\delta$ , and  $\Delta a$ - $\delta$  were shown in Fig. 7. For this concrete material, the tensile strain 0.00025 was assumed a controlling value for distinguishing cracking initiation. On them, the characteristic points were marked after the crack propagation process was carefully investigated.

The crack propagation in some typical loading steps is shown in Fig. 8. At steps 15, and 50 (see Fig. 8 (a) and (b)), the crack propagation increases with increase of load until the maximum load arrives at the loading step 50. When load exceeded its maximum value, the loading began to decrease and the corresponding crack no longer propagates toward the front, and somewhat retrenched backward, see Fig. 8 (c).

In order to observe the stress softening properties on the FPZ, the tensile stress distributions for the several loading states are shown in Fig. 9 (a) and the tensile strain ones in Fig. 9 (b) respectively. They show that although their distributions are somewhat nonlinear, but one could use a bilinear function of the distance from crack tip to approximately characterize the cohesive stress on the FPZ.

Due to great differences between the fracture processes in negative geometry and positive geometry, both the crack initiation and the critical fracture in them are greatly different. Therefore,

nobody has any experience to determine the initial cracking load, critical crack length and the critical fracture load in fracture experiments in negative geometry yet. Through being careful observation of the FPZ, tensile stress and tensile strain distributions and COD on FPZ at the several loading stages, it was found that the crack initiation occurs at the loading step 4, and the critical fracture at the loading step 15. For using the formulae developed in this paper to calculate the double-K fracture parameters, cohesive stress based  $K_R$  curve, net stress intensity factors for the complete loading process, the bilinear softening traction separation law proposed by CEB-FIP Model Code 1990 was employed. In the calculation,  $\sigma_s = 0.368 \text{ MPa}$ ,  $w_s = 0.0613 \text{ mm}$ ,  $w_0 = 0.1 \text{ mm}$  were used.

Through careful investigation, it can be determined that  $P_{mi}$  is 365 N,  $\Delta a_c$  is 83.5 mm and  $P_c$  is 974N. The crack propagation length  $\Delta a_{w_0}$  corresponding to the zero cohesive stress is 140mm. Using the formulae, it can be calculated that  $K_{Ic}^{ini}$  is  $1.218 \text{ MPam}^{1/2}$ ,  $K_{Ic}^{un}$  is  $2.073 \text{ MPam}^{1/2}$ , and  $K_{Ic}^c$  is  $0.810 \text{ MPam}^{1/2}$ . It can be seen that their relation satisfies the three-parameter law of fracture toughness in crack propagation expressed in equation (13) too, for this negative geometry.

In Table 1,  $K^c$  due to cohesive stress,  $K_I$  caused by externally applied load  $P$ , net stress intensity factors  $K_N$  influenced by them common action and the crack extension resistance  $K_R$  based on cohesive stress were shown in columns {5} to {8} respectively. It can be seen that before the critical fracture occurred, the stress intensity factor  $K_I$  caused by the externally applied load  $P$  increases rapidly. During this stage, the crack propagation length increases slowly and the externally applied load increases quickly. As the result, the stress intensity factor  $K_I$  increases rapidly due to the dominance of the loading increase. After the critical fracture load  $P_c$  was exceeded until the maximum load arrived, the stress intensity factor  $K_I$  almost remains constant that is due to the slow ascent of load and observable increase of the crack propagation length. After the maximum load  $P_{max}$  was exceeded, the stress intensity factor  $K_I$  decreases because the load decreased observably and the crack propagation retrenched slightly. The net stress intensity factor  $K_N$  due to the common action of the externally applied load and the cohesive stress shown in column {7} is about 60% of the stress intensity factor  $K_I$  caused by the externally applied load  $P$ . It could be imaged that the zero net stress intensity factor impossibly exists at the fictitious crack tip in concrete

materials for any stage in the complete fracture process.

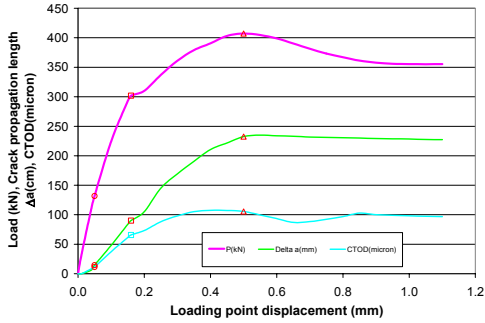


Fig. 7. Plots of P- $\delta$ ,  $\Delta a$ - $\delta$  and CTOD- $\delta$  got in numerical study on an infinite plate with a semi-infinite crack

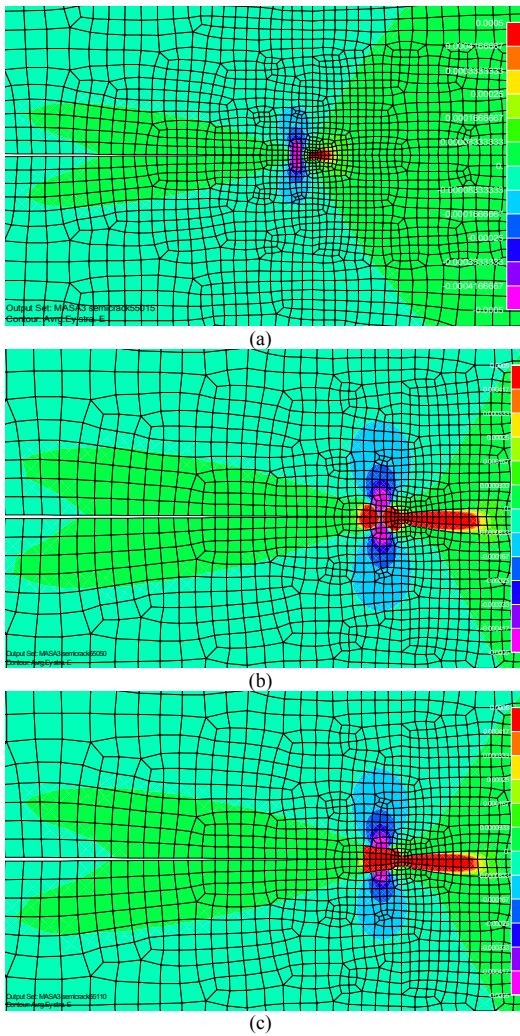
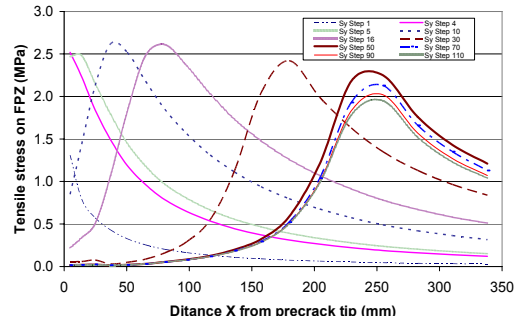
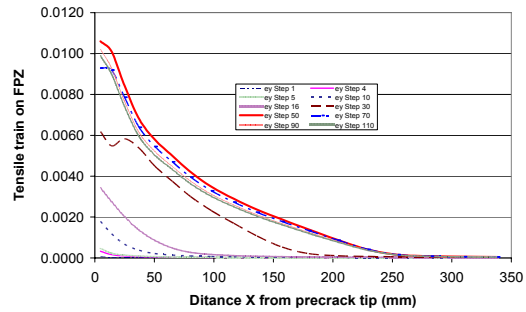


Figure 8 The crack propagation in several loading states.



(a)



(b)

Figure 9 The tensile stress (a) and strain distributions (b) on FPZ.

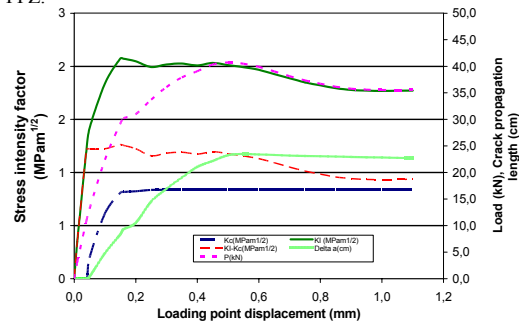


Figure 10 The illustration of P,  $\Delta a$ ,  $K_I$  due to P,  $K^c$  caused by the cohesive stress and the net stress intensity factor  $K_N$  during the complete fracture process in negative geometry

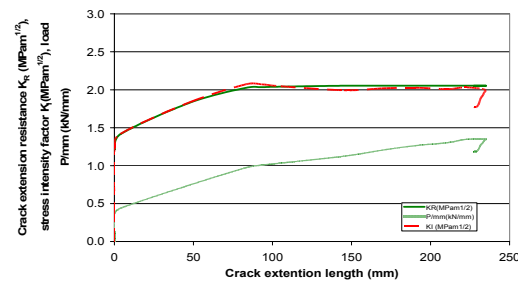


Figure 11 An illustration instance using cohesive stress based  $K_R$  curve compared with the stress intensity factor  $K_I$  curve due to P to describe the crack propagation in negative geometry

Table 1 The results of P,  $\Delta a$ , CTOD,  $K_I$  caused by externally applied load P,  $K^c$  caused by cohesive stress, net stress intensity factors  $K_N$  caused by them common action and the cohesive stress based crack extension resistance  $K_R$

Displacement (mm)	P/mm (N/mm)	a (mm)	CTOD (mm)	$K^c$ (MPam <sup>1/2</sup> )	$K_I$ (MPam <sup>1/2</sup> )	$K_N$ (MPam <sup>1/2</sup> )	$K_R$ (MPam <sup>1/2</sup> )
{1}	{2}	{3}	{4}	{5}	{6}	{7}	{8}
0.010	104.0	0.00	0.0000	0.000	0.347	0.347	1.218
0.040	<b>364.8</b>	0.00	0.0081	0.000	<b>1.218</b>	1.218	1.218
0.050	439.1	3.09	0.0114	0.206	1.428	1.222	1.423
0.100	746.9	40.80	0.0372	0.654	1.904	1.250	1.871
0.150	<b>974.3</b>	<b>83.50</b>	<b>0.0613</b>	<b>0.810</b>	<b>2.073</b>	<b>1.263</b>	<b>2.027</b>
0.160	1006.1	93.00	0.0656	0.819	2.072	1.253	2.036
0.200	1033.4	105.20	0.0732	0.827	2.046	1.219	2.045
0.250	1123.7	145.10	0.0883	0.836	1.994	1.158	2.053
0.300	1203.2	169.30	0.0981	0.836	2.017	1.182	2.053
0.350	1263.7	190.50	0.1051	0.836	2.026	1.190	2.053
0.400	1302.4	210.60	0.1076	0.836	2.008	1.173	2.053
0.450	1344.3	221.60	0.1073	0.836	2.032	1.196	2.053
0.500	<b>1357.2</b>	<b>232.60</b>	<b>0.1056</b>	<b>0.836</b>	<b>2.012</b>	<b>1.176</b>	<b>2.053</b>
0.550	1349.2	235.00	0.0996	0.836	1.992	1.156	2.053
0.600	1329.9	234.00	0.0935	0.836	1.967	1.131	2.053
0.650	1301.2	233.10	0.0870	0.836	1.927	1.091	2.053
0.700	1270.9	231.70	0.0883	0.836	1.887	1.051	2.053
0.750	1244.4	231.10	0.0921	0.836	1.849	1.014	2.053
0.800	1223.7	230.60	0.0968	0.836	1.820	0.984	2.053

All results show that both double-K fracture model and the cohesive stress based  $K_R$  curve method apply to the negative geometry too. The zero net stress intensity factor does not exist at the fictitious crack tip in any stage during the complete fracture process in concrete materials.

## 5. CONCLUSIONS AND DISCUSSION

In this paper, an attempt was made to show whether the double-K fracture model and the cohesive stress based  $K_R$  curve apply to negative geometry based on both analytical investigation and numerical study on the fictitious crack in the infinite plate with a semi-infinite crack. Using the developed analytical solutions and the numerically studied data, double-K fracture parameters, cohesive stress based crack extension resistance  $K_R$ , net stress intensity factor  $K_I$  during the complete fracture process were evaluated and the three parameter law of the fracture toughness increase due to crack propagation was checked once more for the negative geometry. It was found that the fracture toughness increase due to the crack propagation satisfies the three-parameter law for the considered negative geometry, like in positive geometry. The gained results also show that both double-K fracture model and the cohesive stress based  $K_R$  curve apply to the studied negative geometry. Moreover, net stress intensity factor  $K_N$  at the propagating crack tip during the complete fracture process even in negative geometry is significant. Zero net stress

intensity factor at the propagation crack tip in concrete materials is almost impossible.

Acknowledgement: This paper is supported by the National Key Basic Research and Development Program (973 Program) No. 2002CB412709.

## REFERENCES

- Bazant, Z.P. & Oh, B.H. (1983), Crack band theory for fracture of concrete, RILEM, Maters. & Strucs., 16, 155-177.
- CEB-Comite Euro-International du Beton- EB-FIP Model Code 1990, *Bulletin D'Information* No. 213/214, Lausanne, 1993.
- Ozbolt, J, Li Y., Kozar I., (2001), Microplane model for concrete with relaxed kinematic constraint. *Int. J. of Solids and Strucs.*, 38, 2683-2711.
- Tada, H., Paris, P.C. & R. Irwin, G., *The Stress Analysis of Cracks Handbook*. Paris Productions Incorporated, St. Louis, Missouri, USA, 1985.
- Xu, Shilang & H. W. Reinhardt (1998), Crack extension resistance and fracture properties of quasi-brittle softening materials like concrete based on the complete process of fracture. *Int. J. of Fracture*, 92 (1): 71-99.
- Xu, Shilang & H. W. Reinhardt (1999a), Determination of double-K criterion for crack propagation in quasi-brittle materials, part I: experimental investigation of crack propagation. *Int. J. of Fracture*, 98 (2): 111-149.
- Xu, Shilang & H. W. Reinhardt (1999b), Determination of double-K criterion for crack propagation in quasi-brittle materials, part II: analytical evaluating and practical measuring methods for three-point bending notched beams. *Int. J. of Fracture*, 98(2): 151-177.
- Xu, Shilang & H. W. Reinhardt (1999c), Determination of double-K criterion for crack propagation in quasi-brittle materials, part III: compact tension specimens and wedge splitting specimens. *Int. J. of Fracture*, 98 (2): 179-193.
- Xu, Shilang & H. W. Reinhardt (2000), A simplified method for determining double-k fracture parameters for three-point bending tests. *Int. J. of Fracture*, 104 (2): 181-208.